List of Supplementary Materials:

Supplementary Table 1:

Characteristics of human tissue donors of lung tissue used in autoradiography experiments.

Supplementary Table 2:

(Top) Dose-response relationship between the intended exposure produced by the irradiator as compared to the dose detected by TLD.

(Middle) Dose response relationship between intended exposure from irradiator compared to the dose delivered to a simulated lung -simulated mouse body-encased TLD positioned in the shield aperture.

(Bottom) Dose-response relationship between the intended irradiator exposure compared to TLD positioned behind shielding to measure dose delivered to the shielded mouse body.

Supplementary Figure 1:

(Top) Dose response relationship between irradiator exposure and TLD measured dose

(Bottom) Relationship between intended irradiator exposure and delivered dose to unshielded TLD.

Supplementary Figure 2:

In vivo human imaging

Online Supplement

Supplementary Methods:

Murine RILI Model

All experiments and procedures were performed in accordance with the Declaration of Helsinki and the National Institutes of Health's "Guide for the Care and Use of Laboratory Animals" and were approved by the Institutional Animal Care and Use Committee. C57L/J (Stock # 000668) male mice aged 12 weeks (Jackson Laboratories, Barr Harbor, ME) were obtained. A total of 44 mice were used in this study.

Irradiation

Irradiated mice were anesthetized with 87.5 mg/kg ketamine and 12.5 mg/kg xylazine via intraperitoneal injection and secured in custom lead shielding prior to right hemithorax irradiation of 21 Gy via dual source ^{137}Cs Gammacell 40 Exactor (Best Theratronics, Ottawa, Ontario). Following irradiation, animals were returned to their cages and allowed to recover. Mice were kept in a clean animal facility with ad libitum access to food (Purina Test Diet, Richmond, IN USA) and acidified water with 12-hour light/dark cycle. In the losartan treatment groups, mice were allowed ad libitum access to losartan (American Health Packaging, Columbus, Ohio) 40 mg/kg/day dissolved in standard acidified water (vehicle) immediately following irradiation[1, 2]. Water bottles were monitored and refreshed frequently.

Radiation shielding validation

Thermoluminescent dosimeters (TLDs) were used to measure the dose delivered via dual source ^{137}Cs Gammacell 40 Exactor (Best Theratronics, Ottawa, Ontario) to the center of an opening in a custom-made lead shielding apparatus. A series of paired dosimeters were irradiated in the center of the empty specimen cannister of the Cesium irradiator (Supplementary Table 2). Four pairs of TLDs were irradiated over a range of doses from 0.5 Gy to 2.0 Gy, as set by a timer setting on the irradiator calculated from the machine's daily dose rate which is derived from the initial activity of the Cs source and its decay rate. This was done to measure the output of the irradiator and create a dose response curve to characterize how the TLDs record dose in the Cs irradiator in an open configuration. Next a series of paired dosimeters were irradiated in the opening of the lead shielding apparatus. They were enclosed in the center of 1.2 cm thick tissue equivalent material to simulate midplane in a mouse body. This was done for an open configuration dose of 1.0 Gy and 2.0 Gy as prescribed by the timer setting given by the machine's daily dose rate. The ratio of the measured open configuration dose to that of the in-shield dose for a given machine time setting was used to calculate the dose that the mouse lung received, which was 76% of the open field dose (Supplementary Figure 1). From this we infer that a 21 Gy exposure from the irradiator resulted in a 16 Gy tissue dose to the right lung through the aperture of the shielding.

MR Imaging

Imaging protocol as previously described[3]. Briefly, prior to imaging animals were anesthetized with 1–2% isoflurane in 30% oxygen and secured in custom cradle. The tail vein was cannulated and used for injection of probe. Respiration rate was monitored

by a small animal physiological monitoring system (SA Instruments Inc., Stony Brook NY) with target 60 breaths/min. Imaging was performed using a small-bore 4.7 T animal scanner (Biospec, Bruker, Billerica MA) with a custom-built volume coil. T1-weighted (T1w) 3D Ultra Short Time to Echo (UTE) images (repetition time (TR) / echo time (TE) = 4/0.008 ms; flip angle, 5°; field of view, 75 x 75 x 75 mm3; matrix size: 128 x 128 x 128; spatial resolution = 586 µm isotropic; acquisition time, 3 minutes 23 seconds) were obtained prior to and at 20-, 40-, and 60-minutes after the injection of 3 µmol/kg EP-3533. During and immediately following probe injection, a series of 10 T1w 3D Fast Low Angle Shot (FLASH): images (TR/TE = 20/3 ms; flip angle, 12°; field of view, 85 x 65 x 50 mm3; matrix size: 212 x 162 x 100; spatial resolution = 400 x 400 x 500 µm3; acquisition time, 3 minutes 17 seconds) were acquired to monitor probe injection and clearance.

Molecular Probes

EP-3533 comprises a 10–amino acid, disulfide bridged cyclic peptide conjugated to three Gd moieties with affinity for type I collagen (Kd = 1.8 µM) and strong MR signal enhancement (relativity, r_1 = 16.2 $mM^{-1}s^{-1}$ [5.4/Gd ion] at 4.7T), which was synthesized as described previously[4]. ^{68}Ga-CBP8 utilizes the same peptide as EP-3533 but is functionalized with a NODAGA chelator for labeling with Ga-68 A non-binding control probe, ^{68}Ga-Ctrl, was prepared by reduction of the peptide disulfide and alkylation of the thiol groups with iodoacetamide, similarly to a previously described procedure[5]; the resultant linear peptide has negligible affinity for type I collagen[6]. The specificity of EP-3533 for type 1 collagen has been demonstrated *in vivo* previously[3].

Murine MR Image Analysis

Images were analyzed using the program Horos (www.horosproject.org). Regions of Interest (ROI) were identified on the lung, back muscle, and air adjacent to the animal of 5 contiguous slices of pre and post contrast UTE images. Signal intensity (SI) of the lung and muscle of each slice was obtained and standard deviation (SD) of the signal in the air adjacent to the animal was used to estimate noise. For each slice, contrast to noise ratio (CNR) was calculated as follows: $(SI_{lung} – SI_{muscle})/SD_{air}$. An average CNR of all image slices was calculated for the pre-injection images (CNR_{pre}) and for the post-injection images (CNR_{post}) at 20-, 40-, and 60-minutes post injection. The change in CNR, $\Delta CNR = CNR_{post} – CNR_{pre}$, represents lung enhancement due to collagen targeting.

Tissue Analysis

Following imaging, animals were euthanized, and the lungs were harvested. For each experimental condition, a subset of harvested lungs was frozen for molecular analysis. Lung tissue was homogenized and hydroxyproline was quantified by HPLC as previously described[7]. Another subset underwent inflation and fixation of the lungs in neutral 10% buffered formalin, embedded in paraffin, and sectioned into 5 mm-thick slices for hematoxylin and eosin (H&E), Masson's Trichrome, and Sirius red with fast green staining.

Collagen Proportional Area (CPA) and Ashcroft Score:

Sirius red stained slides were digitally scanned and images were analyzed by thresholding to determine the collagen proportional area (CPA), % area stained

collagen positive, using ImageJ (National Institute of Health, Bethesda MD) as previously described[8]. Masson's Trichrome stained sections were analyzed by a pathologist (LH), who was blinded to the study, to score the amount of lung disease via the Ashcroft method[9].

Human Tissue and Autoradiography

With Institutional Review Board approval, remnant human lung resection specimens were obtained from subjects who received radiation therapy for lung cancer (N=3) and nonirradiated control subjects (N=3) (Supplementary Table 1). Tissue was then fixed in OCT and frozen sections 10 µm thick were obtained. Sections were thawed and washed in PBS for 5 minutes three times. The active probe against type 1 collagen, ^{68}Ga-CPB8, and the inactive control probe ^{68}Ga-Ctrl were radiolabeled as described previously[10]. Radioactivity of both probes was quantified using a dose calibrator (Capintec, CRC-55tR, NJ) and found to be similar (1.54 mCi). Tissue sections were incubated with equal radiochemical concentrations of either ^{68}Ga-CBP8 or nonbinding ^{68}Ga-Ctrl for 45 minutes in PBS. The sections were then washed three times with PBS for 5 min. The residual tissue radioactivity was then quantified via Cyclone Plus Phosphor Storage system (Perkin Elmer, Waltham, MA). Analysis performed with Image-J software and quantified with mean arbitrary units.

In Vivo Human Imaging

This study was approved by the Institutional Review Board and registered at clinicaltrials.gov.

Inclusion criteria: Age 18-80, stage I – III NSCLC, received radiation therapy as routine care for lung cancer, diagnosed with radiographically apparent RILI by treating physician.

Exclusion criteria: Subjects were ineligible to participate if: eGFR <30, Stage 4 cancer, pregnant or breastfeeding, BMI >33, known history of pulmonary disease, active smoker, pulmonary infection in past 6 weeks, contraindication to MRI.

PET-MR Imaging Protocol

Subjects provided informed consent. Following a physical exam, a peripheral IV was placed and ^{68}Ga-CBP8 was administered. Approximately 173 MBq (range 148–236 MBq) of ^{68}Ga-CBP8 was administered. Subject 1 received ^{68}Ga-CBP8 while position in the PET-MRI (3 Tesla Biograph mMR, Siemens Healthineers, Erlangen, Germany) to evaluate probe kinetics. All other subjects were placed in the MRI 30 minutes post injection. Simultaneous ^{68}Ga-CBP8 PET and MRI of the thorax was performed. Emission data were acquired for up to 90 minutes in listmode format after the injection of ^{68}Ga-CBP8. Attenuation correction was performed using the manufacturer's MR-based method. Images corresponding to 5-minute dynamic frames were reconstructed using the standard reconstruction algorithm (OSEM, 21 subsets, three iterations, 256 × 256 matrix size,127 slices) and smoothed with a 4-mm full width at half maximum Gaussian filter. Simultaneous to the PET data acquisition the MR data were acquired

with several sequences, including T2-weighted STIR HASTE images acquired coronally during 2 concatenated breath-holds using the following parameters: TE/TR = 100/1000 ms; TI = 0.2 s; flip angle = 120°; reconstruction matrix = 256x179x36, 1.56x1.56x6.9 mm^3; time of acquisition = 36 s. Additionally, dual-echo Dixon images were acquired in order to enable attenuation correction of the PET images, as standard on the mMR scanner, with the following parameters: TE = 1.23/2.46 ms; TR = 3.6 ms; flip angle = 10°; reconstruction matrix = 192x126x128, 2.6x2.6x2.23 mm^3; acquisition time = 19 s. Subjects were contacted the following day to assess for any adverse effects – none reported.

Image analysis

Two independent radiologists reviewed the most recent clinical CT scans of each subject and identified a ROI corresponding to the RILI, and a contralateral ROI of similar size was identified with normal appearing lung. PET signal from 40 to 75 minutes post probe injection was quantified in the ROI's containing both RILI and normal lung. PET signal was binned in 5-minute intervals and quantified in the ROI's containing both RILI and normal lung to provide a washout curve. Blood pool PET signal was quantified in the left ventricle.

Statistics

Statistical analysis was performed using GraphPad (Prism version 6.0). Intergroup analysis performed with one-way ANOVA with post hoc t-test and Bonferroni correction. Area under the curve analysis was performed using the trapezoid method. Strength of linear relationship measured via Pearson correlation. RILI ROI comparison with

contralateral healthy tissue was performed with a paired t-test. *P* value < 0.05 considered significant. Data are reported as mean ± SE.

Supplementary Results:

Supplementary Table 1

Subject	Sex	BMI	Race	Cancer	Stage	Lung	Pk-Yr	CTCAE	Rad type	Dose (Gy)
S1	M	30	Hispanic	S	1A	RUL	30	1	IMRT	59
S2	F	32	Caucasian	S	1A	RML	50	2	SBRT	55
				S	1A	LUL			SBRT	60
S3	F	18	Caucasian	A	1A	RLL	45	1	SBRT	48
				A	1A	LUL			SBRT	50
				A	1A	RLL			SBRT	50
S4	F	23	Caucasian	A	1A	RLL	3	2	SBRT	48
S5	F	22	Asian	A	1B	RUL	2nd hand	1	SBRT	45
S6	F	28	Caucasian	S	3A	RUL	68	3	SBRT	50

Supplementary Table 1**:** Human subjects who underwent imaging with type 1 collagen PET probe. Six subjects were imaged. S2 and S3 had undergone irradiation to multiple tumors and each lesion was analyzed separately to give nine RILI lesions. (S) Squamous cell carcinoma, (A) Adenocarcinoma, (Pk-Yr) smoking pack-years, (CTCAE) Common Terminology Criteria of Adverse Events v5, (SBRT) Stereotactic Body Radiation Therapy, (IMRT) Intensity Modulated Radiation Therapy. No subjects received concurrent chemotherapy.

Supplementary Table 2:

Subject ID	Sex	BMI	Race	Cancer	Stage	Lung	Chemotherapy	Rad type	Dose (Gy)
Control 1	F	25	White	Benign Lesion		LUL			
Control 2	M	24	White	Adenocarcinoma	1A1	RUL			
Control 3	M	25	White	Adenocarcinoma	4	LUL	carboplatin, paclitaxel		
XRT1	M	26	White	Squamous Cell	3A	LLL	cisplatnum, etoposide	SBRT	46
XRT2	F	29	White	Squamous Cell	4	LLL	carboplatin, erbitux, 5FU	SBRT	50
XRT3	F	33	White	Adenocarcinoma	3A	RUL	cisplatinum, pemetrexed	VMAT	50

Supplementary Table 2: Characteristics of human tissue donors of lung tissue used in autoradiography experiments described in Fig 5. “Lung” column describes region of lung where tissue originated from. “Chemotherapy” column reports chemotherapeutic regimens administered prior to biopsy. (SBRT) Stereotactic Body Radiation Therapy, (VMAT) Volumetric Modulated Arc Therapy. Unirradiated “control” subjects (N=3)

Supplementary Table 3:

Unshielded Dose-Response Curve

Dose (cGy)	Replicate	Timer (s)	Dose(cGy)	Reading(cGy)	Avg Reading (cGy)	Sigma (%)	Energy Corrected	Energy and Background Corrected
0	A	0	0	0.04				
	B			0.05	0.04	17.6	0.04	0
50	A	40	50	58.88				
	B			60.3	59.59	1.7	58.42	58.38
100	A	80	100.6	108.21				
	B			106.6	107.4	1.1	105.3	105.26
150	A	120	150.9	166.14				
	B			153.73	159.93	5.5	156.8	156.75
200	A	159	199	224.45				
	B			223.29	223.87	0.4	219.48	219.44

Shielded Dose-Response Curve in Simulated Mouse Body

Dose (cGy)	Replicate	Timer (s)	Dose(cGy)	Reading(cGy)	Avg Reading (cGy)	Sigma (%)	Energy Corrected	Energy and Background Corrected
Shield Aperture								
100	A	80	100.9	75.99				
	B			74.2	75.1	1.7	73.62	73.58
200	A	159	199.9	156.54				
	B			152.47	154.51	1.9	151.48	151.43
200	A	159	199.9	151.53				
	B			148.73	150.13	1.3	147.18	147.14
Shielded								
100	A	80	100.9	3.46				
	B				3.46		3.39	3.35
200	A	159	199.9	6.36				
	B			6.32	6.34	0.5	6.22	6.18
200	A	159	199.9	6.09				
	B			6.08	6.08	0.2	5.97	5.92

Supplementary Table 3: (Top) Dose-response relationship between the intended exposure produced by the irradiator as compared to the dose detected by TLD. (Middle) Dose response relationship between intended exposure from irradiator compared to the dose delivered to a simulated lung -simulated mouse body-encased TLD positioned in the shield aperture. (Bottom) Dose-response relationship between the intended irradiator exposure compared to TLD positioned behind shielding to measure dose delivered to the shielded mouse body.

Supplementary Figure 1

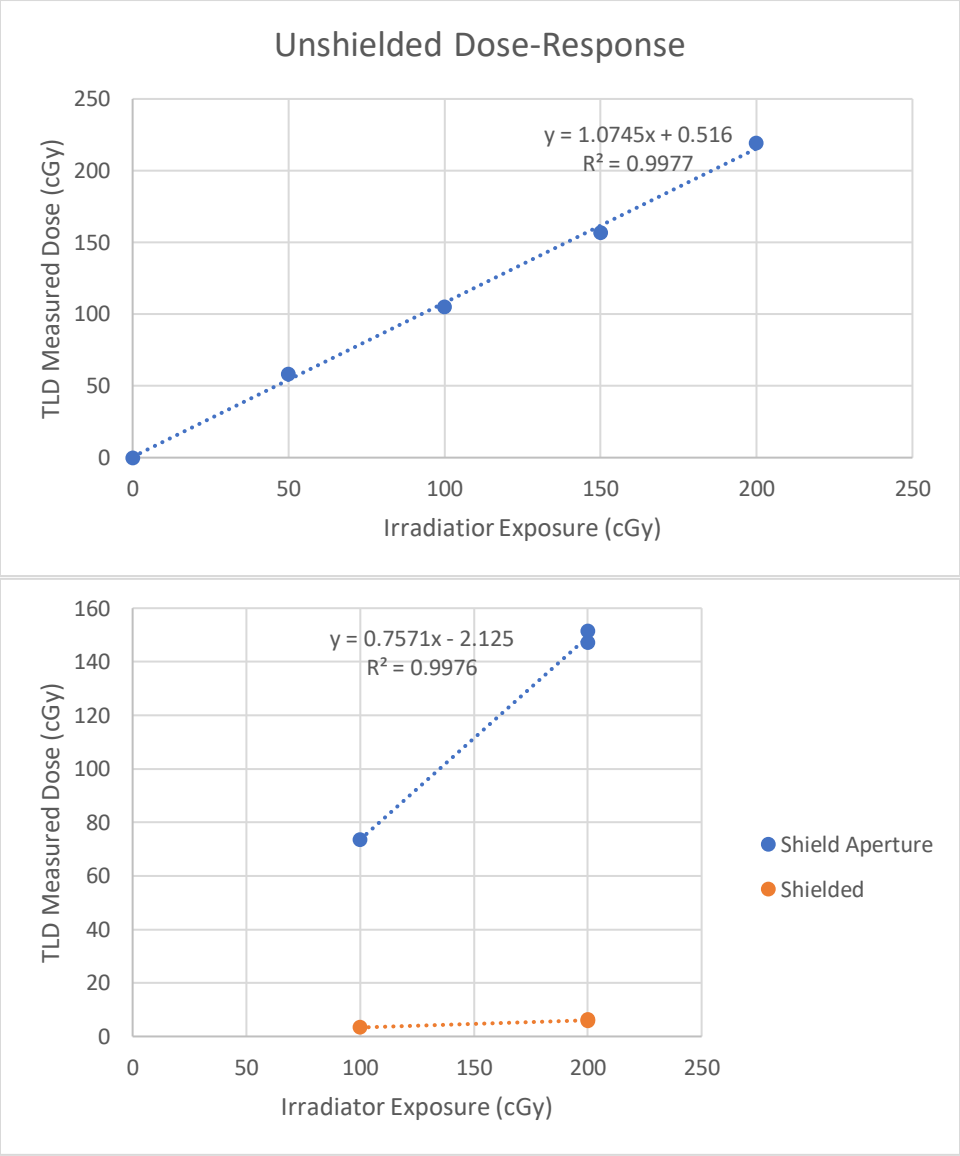

Supplementary Figure 1: (Top) Dose response relationship between irradiator exposure and TLD measured dose. R2 =0.9977, suggesting a close relationship between intended irradiator exposure and delivered dose to unshielded TLD. (Bottom)

Supplementary Figure 2

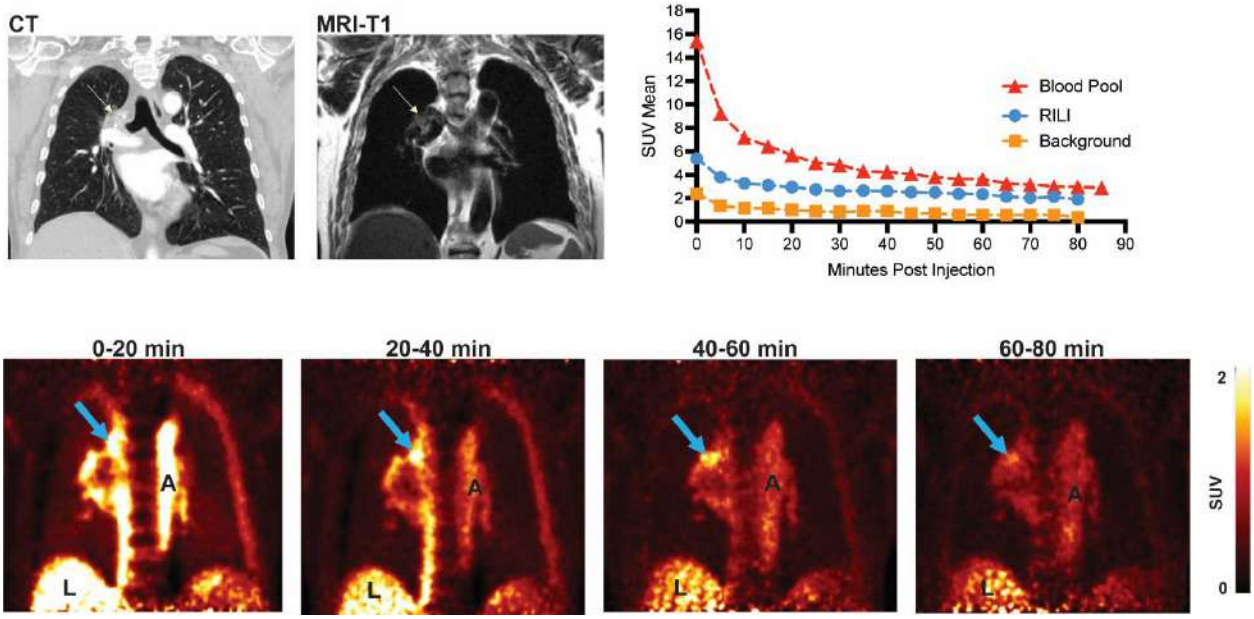

Supplementary Figure 2: In vivo human imaging. Dynamic imaging of ^{68}Ga-CBP8 in a subject with confirmed RILI. (Top row) Coronal HRCT, MR, and PET-MR images. Time activity curves for ^{68}Ga-CBP8 in the blood pool, a region of interest of confirmed RILI and for unaffected lung. (Bottom row) Coronal ^{68}Ga-CBP8 PET images as a function of time demonstrate probe washout. A- Aorta, L – Liver, Arrow – Area of RILI.

References:

1. Zhu BQ, Sievers RE, Browne AE, Lee RJ, Chatterjee K, Grossman W, Karliner JS, Parmley WW, 2003. Comparative effects of aspirin with ACE inhibitor or angiotensin receptor blocker on myocardial infarction and vascular function. J Renin Angiotensin Aldosterone Syst 4: 31-7.
2. Ghosh SN, Zhang R, Fish BL, Semenenko VA, Li XA, Moulder JE, Jacobs ER, Medhora M, 2009. Renin-Angiotensin system suppression mitigates experimental radiation pneumonitis. Int J Radiat Oncol Biol Phys 75: 1528-36.
3. Caravan P, Yang Y, Zachariah R, Schmitt A, Mino-Kenudson M, Chen HH, Sosnovik DE, Dai G, Fuchs BC, Lanuti M, 2013. Molecular magnetic resonance imaging of pulmonary fibrosis in mice. Am J Respir Cell Mol Biol 49: 1120-6.
4. Caravan P, Das B, Dumas S, Epstein FH, Helm PA, Jacques V, Koerner S, Kolodziej A, Shen L, Sun WC, Zhang Z, 2007. Collagen-targeted MRI contrast agent for molecular imaging of fibrosis. Angew Chem Int Ed Engl 46: 8171-3.
5. Overoye-Chan K, Koerner S, Looby RJ, Kolodziej AF, Zech SG, Deng Q, Chasse JM, McMurry TJ, Caravan P, 2008. EP-2104R: a fibrin-specific gadolinium-Based MRI contrast agent for detection of thrombus. J Am Chem Soc 130: 6025-39.
6. Kolodziej AF, Zhang Z, Overoye-Chan K, Jacques V, Caravan P, 2014. Peptide optimization and conjugation strategies in the development of molecularly targeted magnetic resonance imaging contrast agents. Methods Mol Biol 1088: 185-211.
7. Hutson PR, Crawford ME, Sorkness RL, 2003. Liquid chromatographic determination of hydroxyproline in tissue samples. J Chromatogr B Analyt Technol Biomed Life Sci 791: 427-30.
8. Akam EA, Abston E, Rotile NJ, Slattery HR, Zhou IY, Lanuti M, Caravan P, 2020. Improving the reactivity of hydrazine-bearing MRI probes for in vivo imaging of lung fibrogenesis. Chem Sci 11: 224-231.
9. Ashcroft T, Simpson JM, Timbrell V, 1988. Simple method of estimating severity of pulmonary fibrosis on a numerical scale. J Clin Pathol 41: 467-70.
10. Desogere P, Tapias LF, Hariri LP, Rotile NJ, Rietz TA, Probst CK, Blasi F, Day H, Mino-Kenudson M, Weinreb P, Violette SM, Fuchs BC, Tager AM, Lanuti M, Caravan P, 2017. Type I collagen-targeted PET probe for pulmonary fibrosis detection and staging in preclinical models. Sci Transl Med 9.